Proceedings of the 7th International Conference on Civil Structural and Transportation Engineering (ICCSTE'22)
Niagara Falls, Canada – June 05-07, 2022
Paper No. 234
DOI: 10.11159/iccste22.234

Effects of Varying Roof Slope and Wind Direction on Single and Multi-Span Mono-Slope Canopy Roof

Neelam Rani[1], Ajay Pratap[2]
[1]Department of Civil Engineering, Dr. B R Ambedkar National Institute of Technology, Jalandhar, Punjab, India – 144011
ranin@nitj.ac.in; ajayp.ce.19@nitj.ac.in

Abstract - Wind is one of the natural elements that must be addressed while designing structures. The geometry of the roof, the aspect ratio of the building, and the wind direction all influence the actual behaviour of the wind. There are several turbulence effects, particularly near building corners, edges, and roof eaves. Scaled model structures are tested in atmospheric boundary layer wind tunnels to estimate wind pressure coefficients. Experiments in a wind tunnel with scaled building models were carried out in order to estimate the wind pressure coefficients that apply to mono-slope canopy with 0° (flat), 15° and 30° roof slope in this study. Mean wind pressure coefficient is calculated on the upper and lower roof surface of these roof under 0° and 180° wind incidence angle. Further, mean pressure coefficient at the mid-section of mono-slope canopy roof surfaces is represented on the installed pressure points.

***Keywords*:** Single-span, multi-span, mean pressure coefficients, wind tunnel

1. Introduction

Canopy roof (unclad) structures are widely used in places such as railway stations, parking lots, restaurants, sports facilities, bus stops, and solar panel installations [1]. Windstorms usually do the most damage to canopy structure roofs, as it affects both the upper and lower roof surfaces [2] [3] [4] [5]. Current wind load provisions in various national standards, on the other hand, apply to single and multi-span clad buildings [6] [7] [8] [9] [10]. However, there are no guidelines in it for wind loads on multi-span canopy roofs. Even for single span canopy roofs, there is a scarcity of information [11] [12] [13] [14]. As a result, structural engineers have trouble constructing multi-span canopy roofs for various roof shapes. Sometimes, they compromise with the safety of the structure or make it over safe which is not economical. The goal of this study is to evaluate single and multi-span 0°, 15°, and 30° mono-slope canopy roof models in a wind tunnel to measure wind pressure distributions on upper and lower roof surfaces at symmetric (0° and 180°) wind incidence angles.

2. Experimental Investigation

2.1. Wind Tunnel Lab

The tests are being carried out in an open circuit boundary layer wind tunnel at the Department of Civil Engineering at the Indian Institute of Technology Roorkee. Wind tunnel having cross-sectional dimensions of 2 m (width) × 2 m (height) and length section of 15 m. On the upstream end of test section, roughening devices such as vortex generators, barrier walls, and cubical blocks are used to attain mean wind velocity profile equivalent to terrain category 2 as defined by IS 875. (part3) [6] **(see Fig. 1)**. Wind speed inside tunnel alters from 3 m/s to 15 m/s. Turntable of 1.8 m diameter is positioned inside tunnel towards the downstream side, allowing models to be tested in various wind directions. **Fig. 2** shows the profile of mean wind velocity and turbulence intensity observed above the tunnel floor inside the wind tunnel. The reference mean wind speed (U_{ref}) is 6 m/sec measured at a model height of (h_{ref}) 0.075 m and a turbulence intensity of 12% near ground surface to 1% at gradient height. Pressure values are also measured by connecting each pressure point on the instrumented model to the gadget with a plastic tube. The device's one end is connected to pressure tapping, while the other end is attached to a reference pressure point. The wind pressure coefficient (C_P) is calculated by equation 1:

$$C_P = \frac{P-P_0}{0.6\times U_{ref}^2} \tag{1}$$

where, P Static pressure measured at the surfaces on model, P_0 reference pressure measures at reference points, $0.6 \times U_{ref}^2$ dynamic pressure.

2.2. Model details

Single-span scaled model of 1:50 of 0° (flat), 15° and 30° mono-slope canopy roof are created by perspex sheet having same plan dimensions of 0.3 m × 0.15 m and 0.075mm height is taken for investigation as shown in **Fig. (3-4)**. Six columns support the roof: four in the corners and two in the middle of the long edges. Pressure points are given on the model's upper and lower roof surfaces in seven parts, each with five pressure points. A total of 64 pressure points is installed in which upper roof surface has 35 pressure points and lower has only 29 as shown in **Fig. 5**. Due to the existence of supporting columns on the lower side of the roof, the lower surface has fewer pressure points. The model's roof is constructed of two pieces of Perspex sheet with pressure tubing sandwiched between them. Stainless steel pressure tube is first fixed at every pressure point. PVC tubes are attached to it which are then taken down through six supporting columns so that these do not disturb the flow of wind beneath the roof.

Fig. 1: Inside view of the wind tunnel

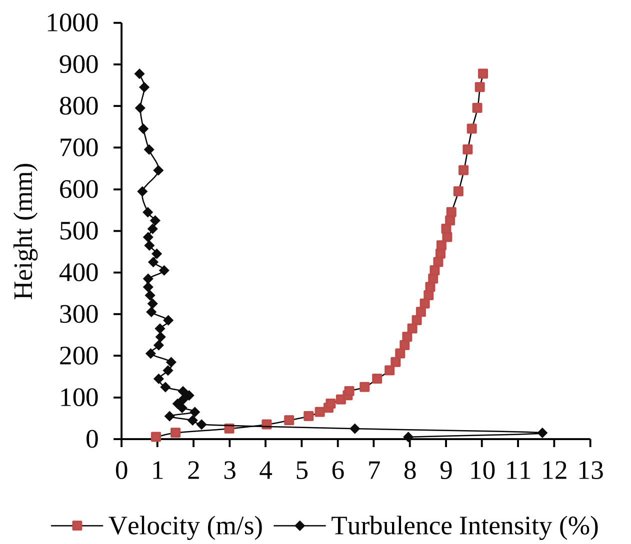

Fig. 2: Wind flow velocity and turbulence intensity profile

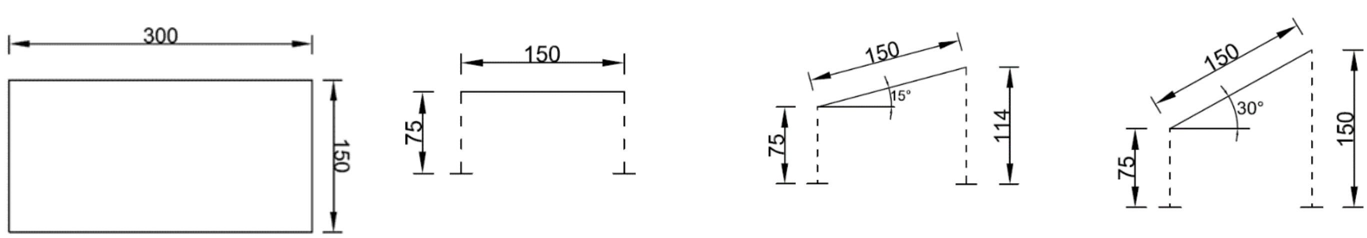

(a) Plan view (b) 0° (flat roof) (c) 15° roof (d) 30° roof

Fig. 3: (a) Plan and elevation view of (b) 0° (flat), (c) 15° and (d) 30° mono-slope canopy roof (all dimensions are in mm)

(a) (b) (c)

Fig. 4: Single span of (a) 0° (flat), (b) 15° and (c) 30° mono-slope canopy roof model kept on turn table inside wind tunnel

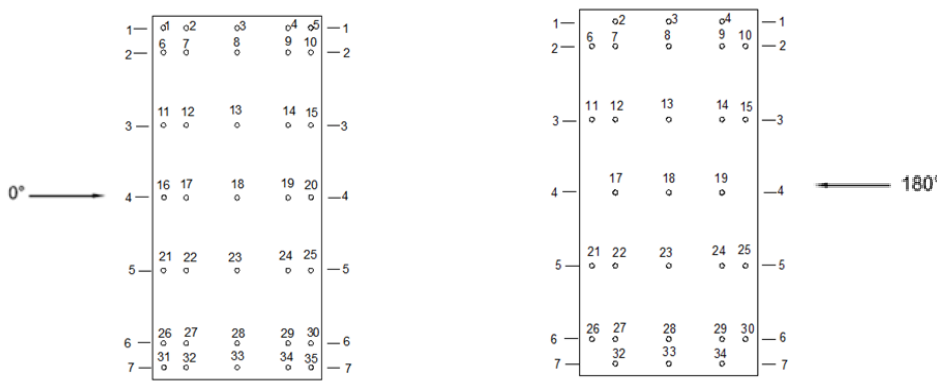

(a) (b)

Fig. 5: Location of pressure points on (a) upper and (b) lower surfaces of mono-slope canopy roof at different sections from (1-1) to (7-7).

To study the wind pressure distribution on multi-span (four span) of 0° (flat) 15° and 30° mono-slope canopy roof, three more dummy models of same dimensions are kept adjacent to the instrumented model (see **Fig.6**). These models are made using plywood and have same dimensions as those of Perspex sheet model. But these are non-instrumented models having no pressure points on it.

(a) (b) (c)

Fig. 6: Multi-span of (a) 0° (flat), (b) 15° and (c) 30° mono-slope canopy roof model kept on turn table inside wind tunnel

2.3. Measurement technique

The effect of wind pressure is measured under wind incidence angle of 0° and 180°. Flat canopy roof is symmetric about its geometrical axis so, 0° and 180° wind incidence angle give same value of pressure coefficient. The direction of wind angle is shown in **Fig. 7** for single and multi-span buildings.

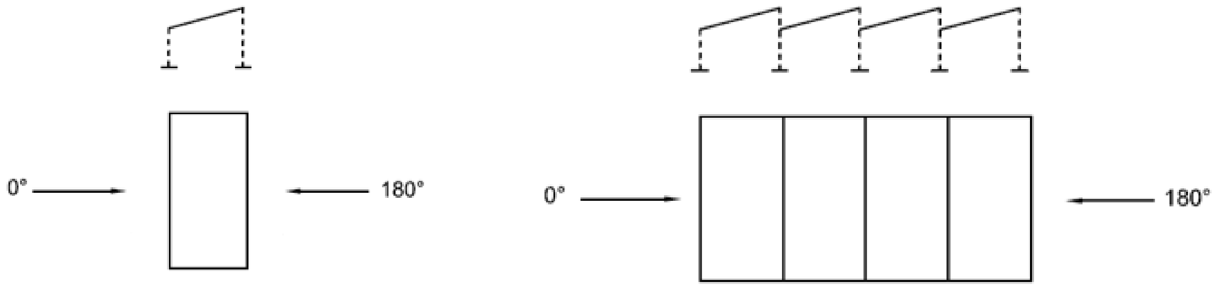

Fig. 7: Wind incidence angle for (a) single span and (b) multi-span (four span)

The instrumented model of the single span 0°, 15° and 30° mono-slope canopy roof is placed at the centre of turn table in such a way that wind hits perpendicular to the long edge of the model. This orientation is considered as 0° wind incidence angle. At this angle of attack, pressure points no. 1, 6, 11, 16, 21, 26 and 31 fall on windward side (see Fig.5(a)). Wind pressure readings are taken at pressure locations on the model's upper and lower roof surfaces. The turntable is spun 180° after monitoring the pressures at a 0° wind incidence angle to examine the wind load effect in this direction.

To measure wind pressure distribution on multi-span (four span) of 0°, 15° and 30° mono-slope canopy, first of all instrumented model is placed at the centre of the turn table inside the wind tunnel in such a way that pressure points no. 1, 6, 11, 16, 21, 26 and 31 fall at the windward side. Other three dummy (non-instrumented) models are placed adjacent to the instrumented model. Measurement of the wind pressure distribution is made at all pressure points on the upper and lower roof surface. Later, last non-instrumented model is removed from its position and placed on upstream side of the instrumented model in such a way that instrumented model comes in second position to the direction of wind with one non-instrumented model on upstream side and other two non-instrumented models on downstream side of it (see **Fig. 8**).

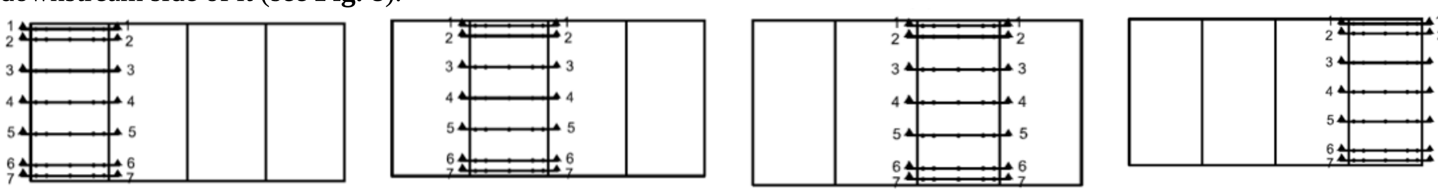

(a) (b) (c) (d)

Fig. 8: Wind pressure calculation on (a) First, (b) Second, (c) third and (d) fourth (multi-span) span canopy roof at different sections under 0° and 180° wind angle.

3. Results and Discussion

3.1. Single-Span

Mean pressure coefficient ($C_{p,\ mean}$) distribution on the upper and lower surface of single-span for 0°, 15° and 30° mono-slope canopy roof surfaces under 0° and 180° wind angle is shown as contour lines in **Fig. 9**. Symmetry in the $C_{p,\ mean}$ distribution along the mid-axis (section 4-4) can be observed clearly. $C_{p,\ mean}$ values are more on the upper and lower surface at the windward region whereas it decreases along the leeward surface region. This is expected because the flow separates at the windward region when it strikes with the windward surfaces, and it accelerates at the edges and then it starts decelerating along the panel surfaces.

Roof	**Wind incidence angle**	**Upper roof surface**	**Lower roof surface**

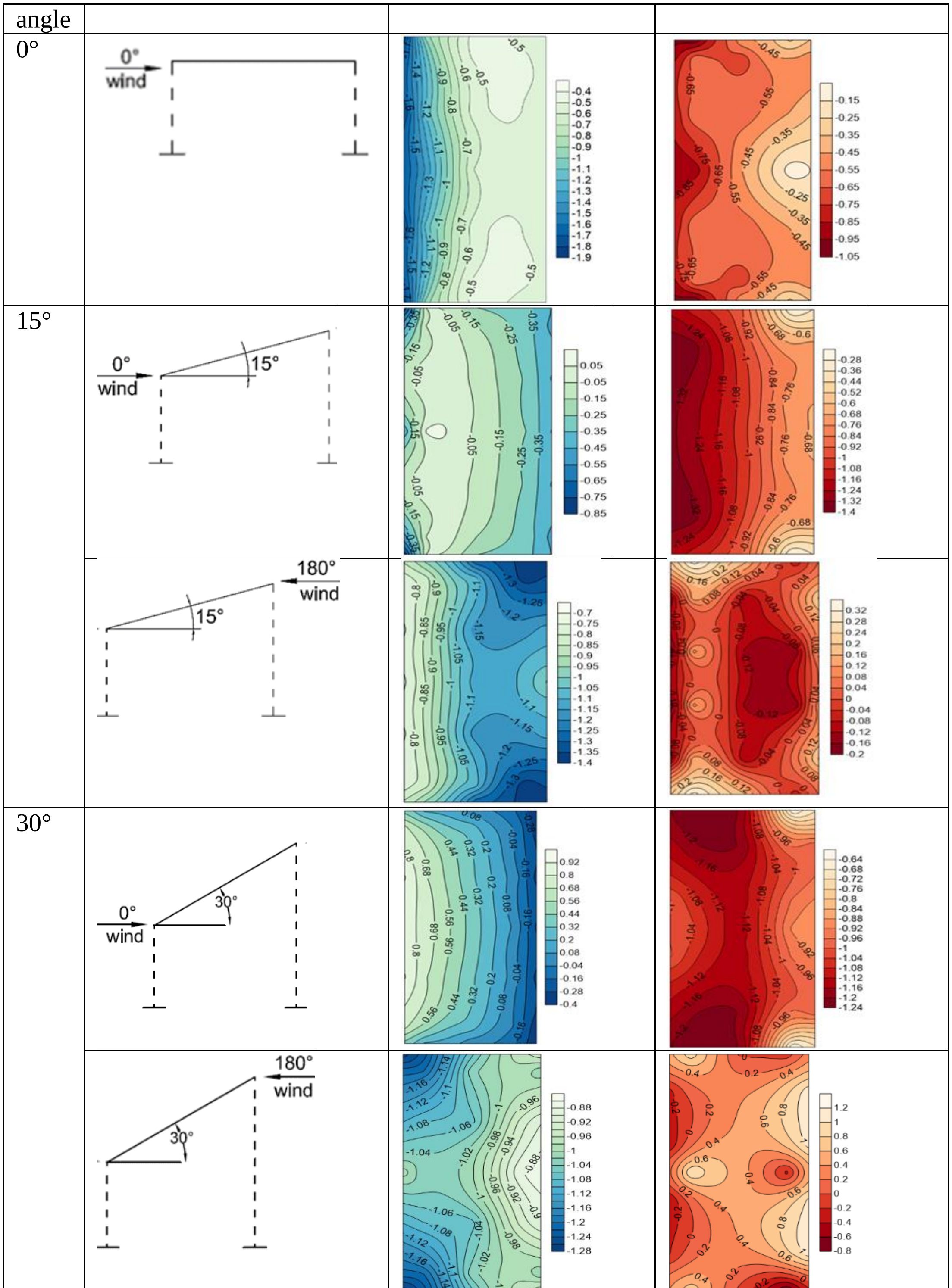

Fig. 9: Contour mean wind pressure coefficient on upper and lower surfaces of 0°, 15° and 30° mono-slope canopy roof under 0° and 180° wind angle.

For 0° and 180° wind angle, the magnitude of $C_{p,\ mean}$ decreases on the upper surface whereas it increases on the lower surfaces as roof slope increases as wind moves from windward to leeward side. Localized maximum and minimum pressures are seen close to the leading edge of the panel at certain wind angles, with a decrease towards the trailing edge.

3.1. Multi-Span (Four Span)

Variation of $C_{p,\ mean}$ obtained from testing on the installed pressure points at mid-section (4-4) on upper and lower surface of 0°, 15° and 30° mono-slope canopy roof under 0° and 180° wind angle is illustrated in **Fig (10-13)**. For 0° roof, $Cp_{,\ mean}$ shows higher magnitude on upper and lower surfaces at the edges of windward span (first) and then it decreases drastically for remaining spans. Second, third and fourth span shows almost similar values of $C_{p,\ mean}$ at section (4-4) on both upper and lower roof surfaces (see **Fig. 10**).

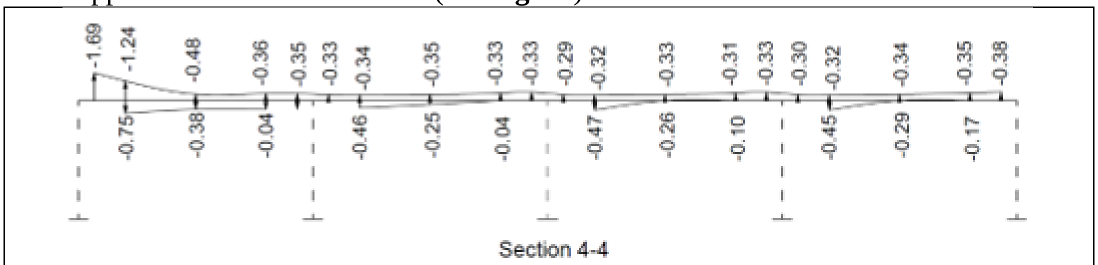

Fig. 10: Variation of $C_{p,\ mean}$ on upper and lower surfaces of 0° roof for 0° wind incidence angle

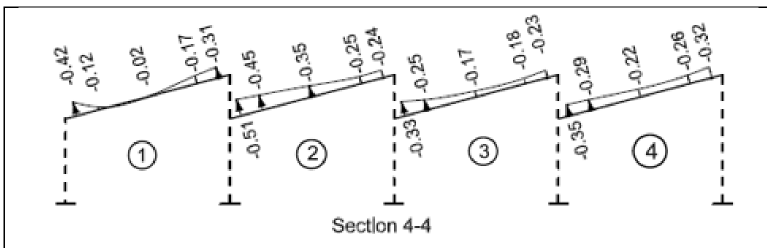

(a)

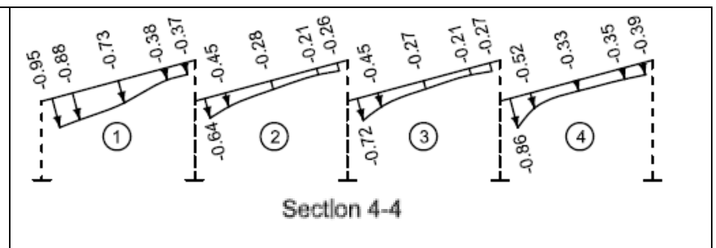

(b)

Fig. 11: Variation of $Cp_{,\ mean}$ on (a) upper and (b) lower roof surface of four span mono-slope canopy of 15° roof for 0° wind incidence angle

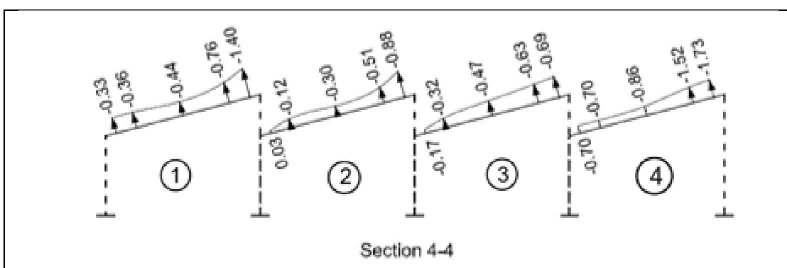

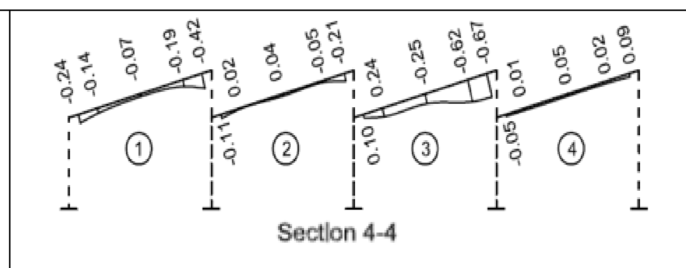

Fig. 12: Variation of $Cp_{,\ mean}$ on (a) upper and (b) lower roof surface of four span mono-slope canopy of 15° roof for 180° wind incidence angle

In case of 0° wind incidence angle for 15° roof, $Cp_{,\ mean}$ on lower surfaces shows higher magnitude at the edges of windward span (first) and then it decreases for remaining spans whereas second span of upper surface shows more value as compared to first span and then it becomes similar third and fourth span (see **Fig. 11**). In case of 180° wind incidence angle, upper roof surfaces show higher magnitude of $Cp_{,\ mean}$ at the windward surfaces (fourth span) further, it decreases for remaining span whereas on lower surfaces magnitude of $Cp_{,\ mean}$ shows less value at windward face and maximum value for leeward span (first) (see **Fig. 12**).

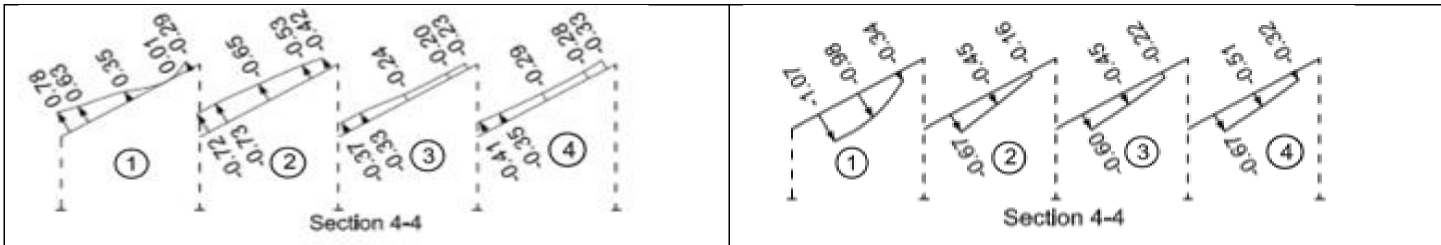

(a) (b)

Fig. 13: Variation of $Cp_{,\ mean}$ on (a) upper and (b) lower roof surface of four span mono-slope canopy of 30° roof for 0° wind incidence angle

In case of 0° wind incidence angle for 30° roof, $Cp_{,\ mean}$ distribution shows similar trend on upper and lower surfaces of 15° roof as discussed earlier (see **Fig. 13**).

4. Conclusion

It was observed from the study that in case of symmetric wind angle along the geometrical axis of single span model there is uniform distribution of wind pressure coefficient on the surfaces of mono-slope canopy roof. For 0° and 180° wind angle, the magnitude of $C_{p,\ mean}$ decreases on the upper surface whereas it increases on the lower surfaces as roof slope increases as wind moves from windward to leeward side. The localized wind pressure is maximum close to the leading edge of the mono-slope canopy roof for wind directions studied here. Largest suction (negative pressure) exists along the roof edges and corners of roof surfaces due to flow separation region. In case of multi-span mono-slope canopy model $Cp_{,\ mean}$ is predominant up to first and second span of windward side and then it reduces for remaining span.

Acknowledgements

The authors wish to acknowledge the generous support of Department of Civil Engineering at Indian Institute of Technology Roorkee's in providing graduate assistant support.

References

[1] B. Natalini and M.B. Natalini, Wind loads on buildings with vaulted roofs and side walls – A review, J. Wind Eng. Ind. Aerodyn. vol. 161, pp. 9–16, 2017.

[2] C.W. Letchford and J.D. Ginger, Wind loads on planar canopy roofs - Part 1: Mean pressure distributions, J. Wind Eng. Ind. Aerodyn. vol. 45, pp. 25–45, 1992.

[3] B. Natalini, J.O. Marighetti, M.B. Natalini, Wind tunnel modelling of mean pressures on planar canopy roof, J. Wind Eng. Ind. Aerodyn. Vol.90, pp. 427–439, 2002.

[4] A.K. Roy, A. Aziz, S.K. Verma, S.K. Sharma, Influence of Surrounding Buildings on Canopy Roof of Low Rise Buildings in Abl By Cfd, (2018).

[5] J. Wang, Q. Yang, Y. Tamura, Effects of building parameters on wind loads on flat-roof-mounted solar arrays, J. Wind Eng. Ind. Aerodyn. vol.174, pp. 210–224, 2018.

[6] IS: 875 (Part-3), Code of Practice for Design Loads (other than Earthquake Loads), for Building and Structures – Wind Loads, 2015.

[7] BS 6399-2:, Loading for buildings Part 2. Code of practice for wind loads, 1997.

[8] AS/NZS: 1170.2, Australian/New Zealand Standard: Structural Design Actions Part-2: Wind Actions, 2002.

[9] EN: 1991-1-4-2005, Euro Code 1: Actions on Structures– Wind Actions, 2011.

[10] ASCE:7-98, American Society of Civil Engineers (ASCE), 2013.

[11] M.B. Natalini, C. Morel, B. Natalini, Mean loads on vaulted canopy roofs, J. Wind Eng. Ind. Aerodyn. vol. 119 pp. 102–113, 2013.
[12] A.K. Roy, A.K. Ahuja, V.K. Gupta, Variation of wind pressure on Canopy-Roofs, Int. J. Earth Sci. Eng. vol.03, pp.19–30, 2010.
[13] Y. Uematsu, R. Yamamura, Wind loads for designing the main wind-force resisting systems of cylindrical free-standing canopy roofs pp. 125–143, 2019.
[14] N.S. Fouad, G.H. Mahmoud, N.E. Nasr, Comparative study of international codes wind loads and CFD results for low rise buildings, Alexandria Eng. J. vol. 57, pp. 3623–3639, 2018.